

PAPER • OPEN ACCESS

Necessary measures and calculation for dimension of coaxial heat exchanger for deep boreholes

To cite this article: V Stefanovi *et al* 2019 *IOP Conf. Ser.: Mater. Sci. Eng.* **477** 012054

View the [article online](#) for updates and enhancements.

Necessary measures and calculation for dimension of coaxial heat exchanger for deep boreholes

V Stefanović¹, B Drobñjaković² and S Pavlović¹

¹Faculty for Mechanical Engineering Niš ,Aleksandra Medvedeva Street,18000, Niš, Srbija

²Institute for Mining and Metallurgy Bor, Zeleni bulevar Street, 19210 Bor, Srbija

E-mail: bojan.drobñjakovic@irmbor.co.rs

Abstract. This paper aims to illustrate the complexity of the approach to modeling a potential heat exchanger envisaged for deep drilling. The problem was presented in one example of the installation study for the heating and cooling of the University building in the city of Aachen, Germany, with a deep coaxial heat exchanger, located in a depth well of 2500m (BHE). Prior to any modelling of the heat exchanger, the geological analysis of the wall layers along the well was to be approached; to conduct complex field and laboratory geophysical measurements and ultimately to approximate the modeling of heat processes in the heat exchanger. Also, this study was aimed at assessing the feasibility of such an installation for heating and cooling space, as well as clarifying operational characteristics and performance (in the long run). Direct heating of the building in the winter period requires a temperature of 40°C. In the summer period, for the cooling of the university building, an adsorption cooling unit is used, which requires a temperature of at least 55°C. Dredged walls up to a depth of 2500m have extremely low permeability and porosity, less than 1%. Their thermal conductivity varies between 2.2W/(mK) and 8.9W/(mK), more values are associated with quartz sandstone. The maximum temperature in the well is 850C at a depth of 2500m, corresponding to a mean specific heat flow of 85mW/m2-90mW/m2. The experience of twenty years of work has indicated that only in a short period of time, the borehole can supply the desired temperature for the operation of the absorption refrigerant. In winter, the heat exchanger can also supply a building with sufficient heat.

1. Introduction

Much before 2004, it is planned that in the framework of the Aachen unification, a deep well will be built in which a heat exchanger (BHE) will be installed, for the use of geothermal energy for heating and cooling the new building of the student center, which is classified into the energy class "Super C". In the summer period, a large roof area should provide shade, while in winter it is necessary to provide passive heating by solar radiation through glass surfaces. Solar cells on the roof should generate electricity for the needs of a circulation pump for a heat exchanger [1].

A deep coaxial heat exchanger is a closed system where cold water flows through the outer tube, heats up, enters the inner tube and flows upwards. The borehole under the official name RWTH-1 has a depth of 2500m and is intended to provide heat for heating and cooling through BHE. The outlet water temperature from the inner tube of the exchanger should have a temperature of at least 55°C-80°C. In order to operate an absorption cooling system during the flight, a minimum temperature of 55°C is



required. A period of 30 to 40 years is foreseen. In winter, the building will be heated directly by geothermal heating water. The well was drilled in the spring of 2004, before the construction of the university building (Figure 1). The building is located in the urban part in the center of Aachen. The drilling operation was monitored from the petrographic side and the temperature side. The bore is crossed by a wall series dominated by sandstone and gravel. Organic gravel and thin coal layers were locally found in the upper half to 1016 m as part of the carbonic delta cycles. From limestone 1016m to 1440m, limestone walls from the period of the Upper Devon dominate. In the deeper part of the well, dominant shale and series of sandstones date from the period of the lower devon [2]. During the drilling, material from the drilling rig was sampled (Figure 2), length 1m. Cores samples were available for 3 sections along the well (1391.5m-1515.7m, 2128.2m-2142.8m and 2536.8m-2544.5m) with a total length of 150m samples of the core. No fluid flow into the well was detected during drilling. The most important information needed on the walls for long-term simulation of the heat exchanger's performance in deep wells is the thermal conductivity of the wall material, then the specific heat capacity, porosity, permeability and density [3].

The building is located in the urban part in the center of Aachen. Borehole is in the red circle.

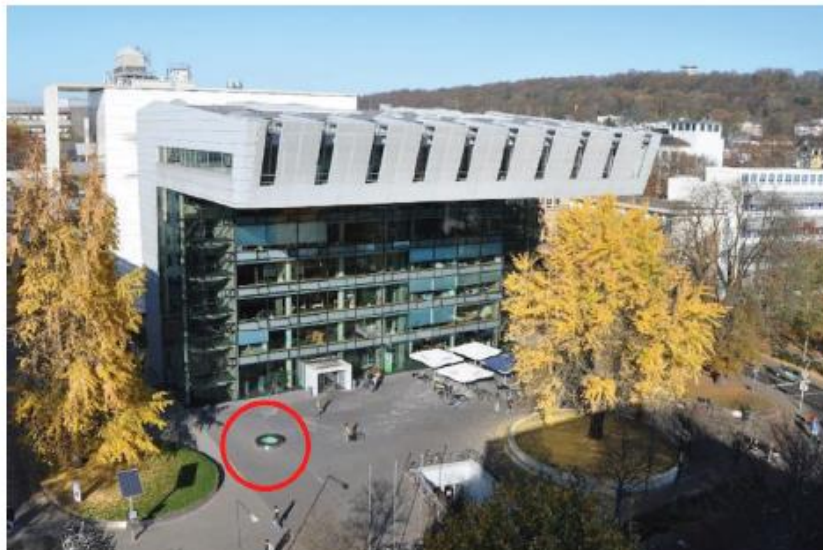


Figure 1. Building "Super C" energy class

2. Necessary measures

This section will show the required measurements.

2.1. Laboratory Measurements

Necessary physical measurements are measurements of density and thermal conductivity of layers; 57 samples were selected at intervals of 50m in depth, from the walls considered to vary in geophysical terms. The density of the pm core was measured (Figure 2) with helium pycnometer [4]. The device calculates the density of the matrix over the amount of helium that saturates the pores in the dried core sample. The density varies from 2640 kg/m^3 to 2840 kg/m^3 , the mean value is 2780 kg/m^3 . The accuracy of the device for the increase of 1 kg/m^3 is $0,1 \text{ kg/m}^3$. Bulk density can not be measured because only core samples from the most stable, massive parts of drilled walls were available.

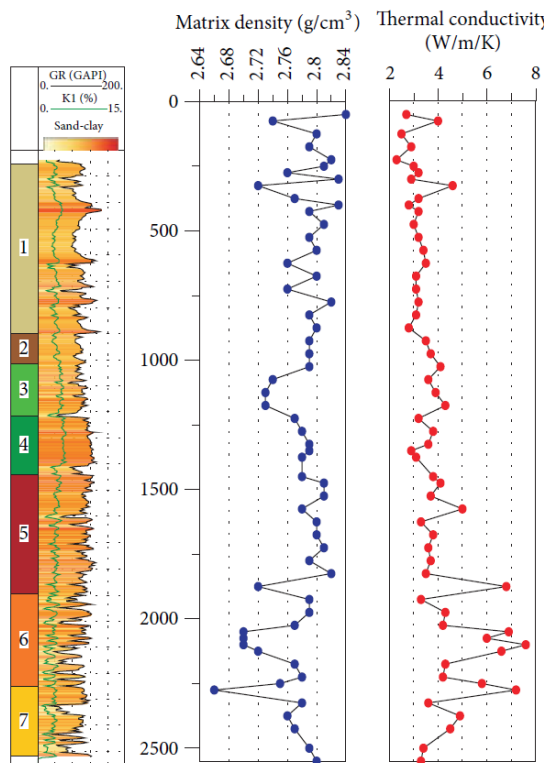


Figure 2. Density and heat measurements conductivity in the borehole zones

The core density is measured with a multisensor logger, and on some cores with a helium gas pycnometer. The multisensor logger uses the source of gamma radiation and measures the intensity of gamma radiation. The density is calculated from the absorbed gamma radiation. The process requires careful calibration of the measuring device. The density of helium gas pycnometer measured varies between 2391kg/m^3 and 2897kg/m^3 , on average 2820kg/m^3 . The density of gamma measurements varies between 2576kg/m^3 to 3233kg/m^3 , on average 2830kg/m^3 .

Thermal conductivity of the core (Figure 2) was measured using a TK04 needle probe (TeKa Geophysical Instruments product) in a mixture of the core with water. The thermal conductivity of the samples varies from 2.2W/(mK) to 8.9W/(mK) , on average 3.8W/(mK) . High values can be explained by a high percentage of quartz. Cemented quartz sands often appear in the deeper part of the well below 1895m [2].

The thermal conductivity of the core was measured using the Thermal Conductivity Optical Thermal Scanner (TCS) manufactured by Lippmann & Rauhen GbR [5]. The thermal conductivity scanner moves along the sample, detects the heat radiation of the sample, and calculates the heat conductivity of the sample with an error of $\pm 3\%$ at measured temperatures before and after scanning. The thermal conductivity of the core varies between 2.3W/(mK) and 4.9W/(mK) with minimum values of 2.0W/(mK) and a maximum of 5.9W/(mK) . The arithmetic mean is 3.02W/(mK) , as well as the geometric mean 2.99W/(mK) , [6].

Additional sizes measured on the core with a multisensor logger are density, porosity, magnetic sensitivity, sound velocity and natural gamma radiation. Due to their low porosity, no differences in the saturated and dry samples of the core were detected between them. The porosity (ϕ) of the three selected core samples was calculated according to the quantity of water that evaporates from the sample. Porosity is almost zero, with a mean value of 0.012% .

2.2. Measurements in the borehole

The measured temperature logs are shown in Figure 3. The first measurements of temperature in April 2005 show higher temperatures in the upper half of the wells and lower temperatures in the lower half

of the well compared to the June 2006 measurements. This is probably caused by the influence of drilling fluid; which heats the upper part and cools the bottom of the well during drilling. In the first 50m, the temperature anomaly occurs in both temperature curves. This is unusual, but can be explained by the thermal losses of drilling water in higher permeable sediments at the top of the well due to the cooler wall mass. Measurement of density with radioactive source was not done because it was the center of the city of Aachen. The sound velocity V_p , electrical resistance, and gamma radiation are shown in Figure 4. Logs of the measured gamma radiation are used for geological interpretation in the section. Gamma radiation gives an indication of the clay content in the wall. Therefore, these data are used to determine thermal conductivity and radiological heat generation. V_p data (logging data) are compared with core data (black line versus blue line "log /Core V_p " in Figure 3). Data "in city" and data from the laboratory fit perfectly. The results best suit the limestone part up to 1440m and in the cores from the deepest part of section 1. Between 1460m and 1490m a slight deviation can be observed, which can be attributed to an anisotropic environment.

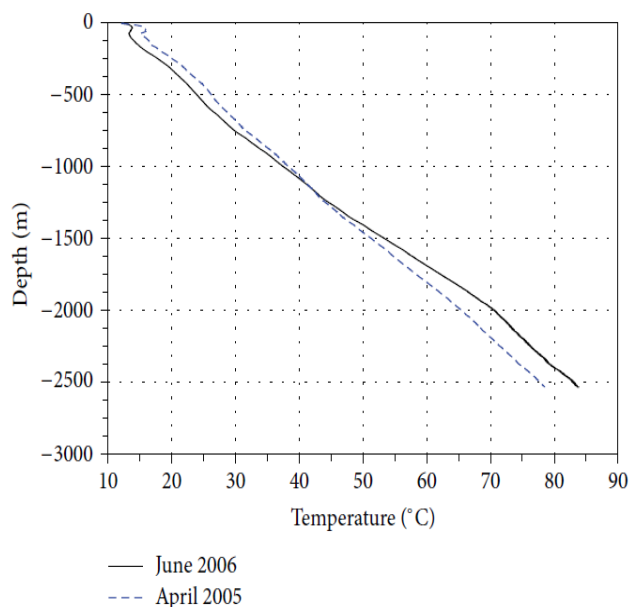


Figure 3. Temperature diagram in the borehole in different periods of time

2.3. Interpretation of log records

Based on the recorded geological data, the well profile is divided into three larger zones (Figure 4): (I) zones of lower limestone delta layers, (II) zones of the upper devon layers, clay stone, limestone sandstone and limestone and zones (III) with a fairly homogeneous succession of sand and clay stone of the lower Devonian era (Figure 4).

The value of the logarithm of electrical resistance reaches values of up to 1000Ω for limestone and quartz cement sand, while the organic shards have a resistance lower than 100Ω.

2.4. Heat Characteristics

It is not possible to measure the thermal conductivity directly in the well, so that it is necessary to find existing logs for determining thermal conductivity. The content of clay volume was derived from the contribution of potassium as a whole to gamma radiation. As described in the previous section, the well was divided into 7 zones.

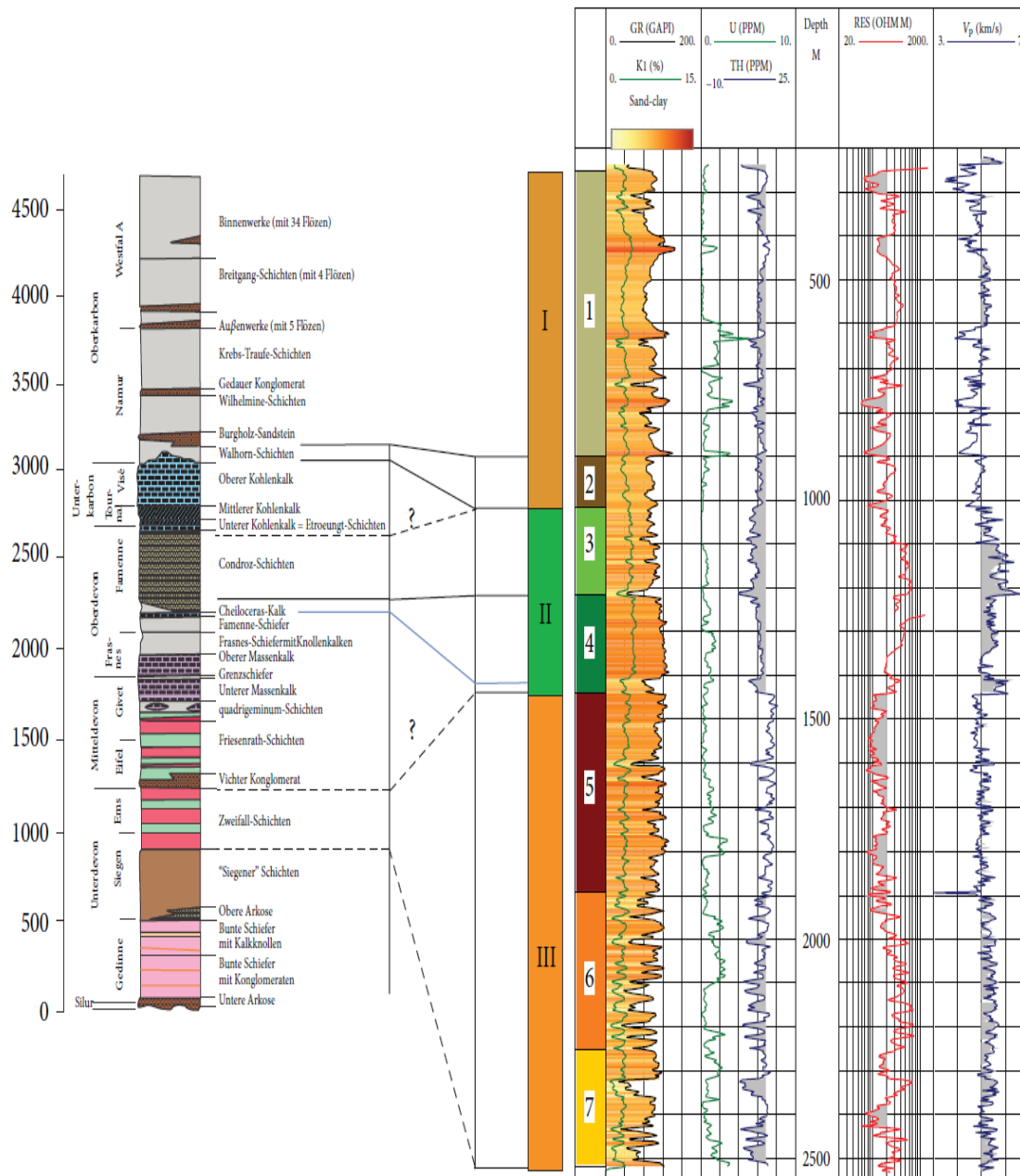


Figure 4. Geological zoning of the borehole [2]

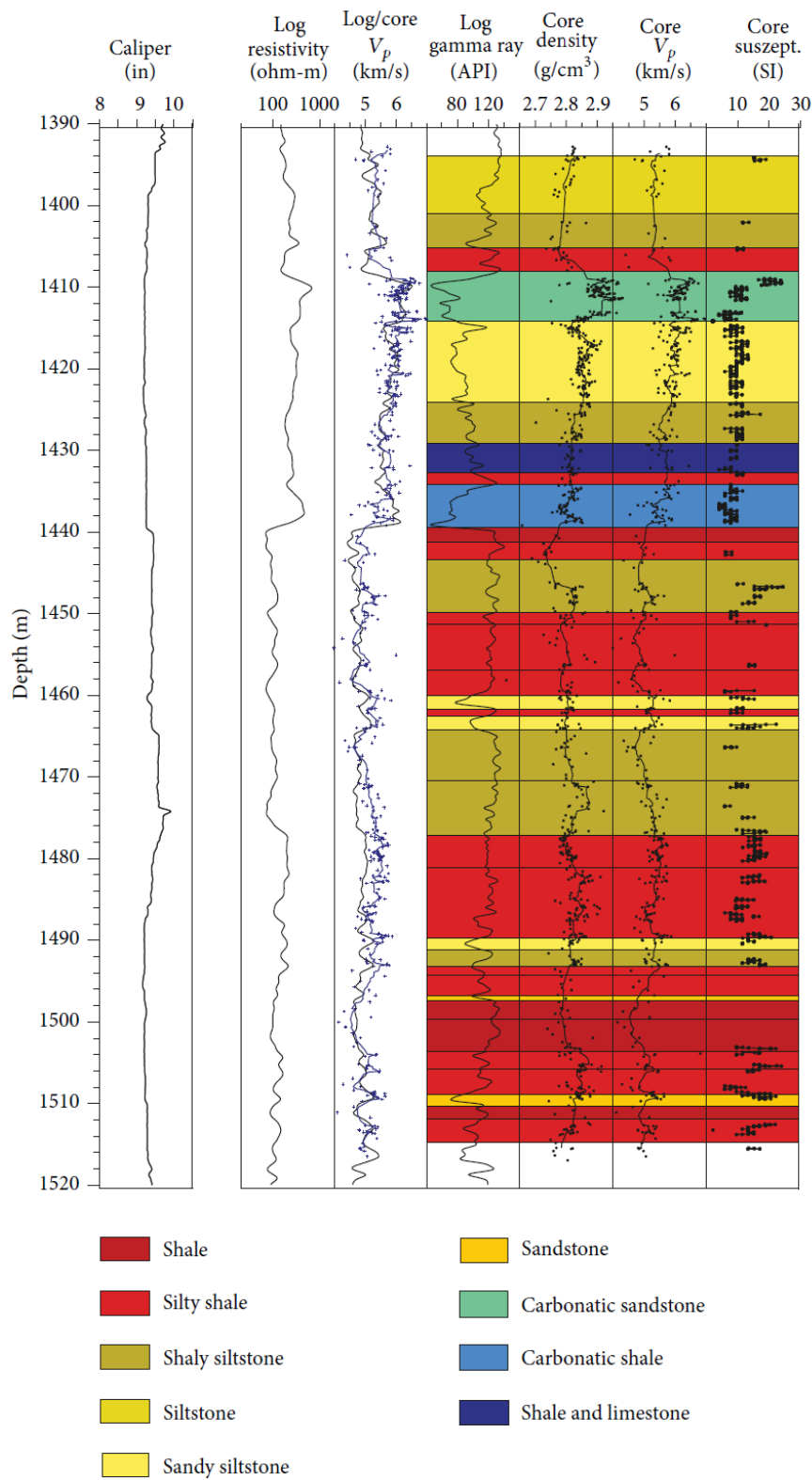


Figure 5. Petrography data on cores by zones. Colors indicate the type of wall according to the petrography description of the core [2]

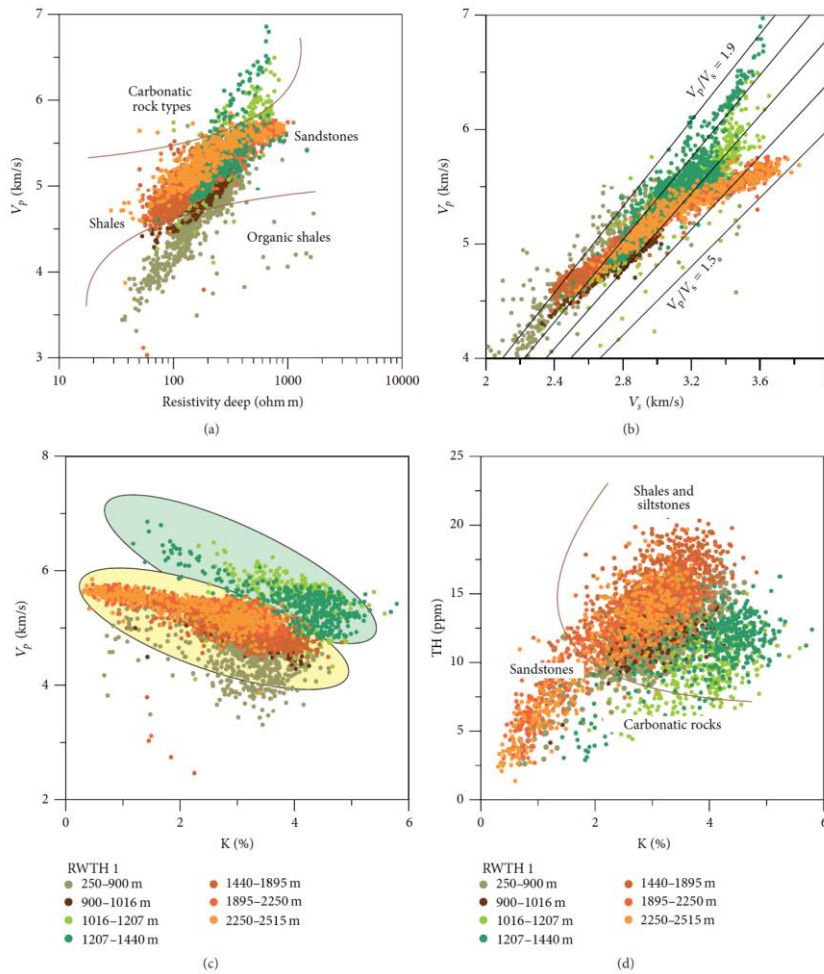


Figure 6.

Because of the paleo compensation and post-experimental processes, the ratio of natural gamma activity to relative volume of clay differs between these areas. This segmentation allows the continuous thermal conductivity of the entire profile along the depth of the well, using a natural gamma log for each individual zone and calibrating with thermal conductivity measured on a charged core [6].

The rate of compression and the effect of gamma radiation of the potassium substance were used to identify 7 zones with a defined content of 100% clay. Assuming that clay is the only source of relevant potassium radiation, 0% of the clay is assigned to the lowest total value. Identification of thermal conductivity λ_1 on a scale with clay content and thermal conductivity λ_2 on quark scale with the rest of the wall gives the thermal conductivity of λ_{log} . The log (log) has a vertical resolution of 0.076m and the values are harmonized at an interval of 2m. In order to calculate the heat conductivity, the arithmetic (AM) and geometric (GM) mean were used:

$$\lambda_{AM} = \lambda_1 V_{clay} + \lambda_2 (1 - V_{clay}) \quad (1)$$

$$\lambda_{GM} = \lambda_1^{V_{clay}} \lambda_2^{(1-V_{clay})} \quad (2)$$

For each pre-identified zone, the thermal conductivity is conditioned by the clay content in the rest of the wall. For each measured value on the sample, the corresponding log value (log) was identified.

Calculated λ_{\log} were adjusted to the measured changes λ_1 and λ_2 [6]. This resulted in thermal conductivity logs (Figure 7). "TC AM" is based on the arithmetic mean of λ_{\log} calibrated by minimizing the variance between λ_{\log} and the measured value. "TC GM" is based on the geometric calibration method λ_{\log} by minimizing the minimum square deviation between λ_{\log} and the measured values. In addition, the continuous profile of heat production through the entire well was derived from the sound record [7], [8] and the spectral gamma log [9]. The results are shown in Figure 7.

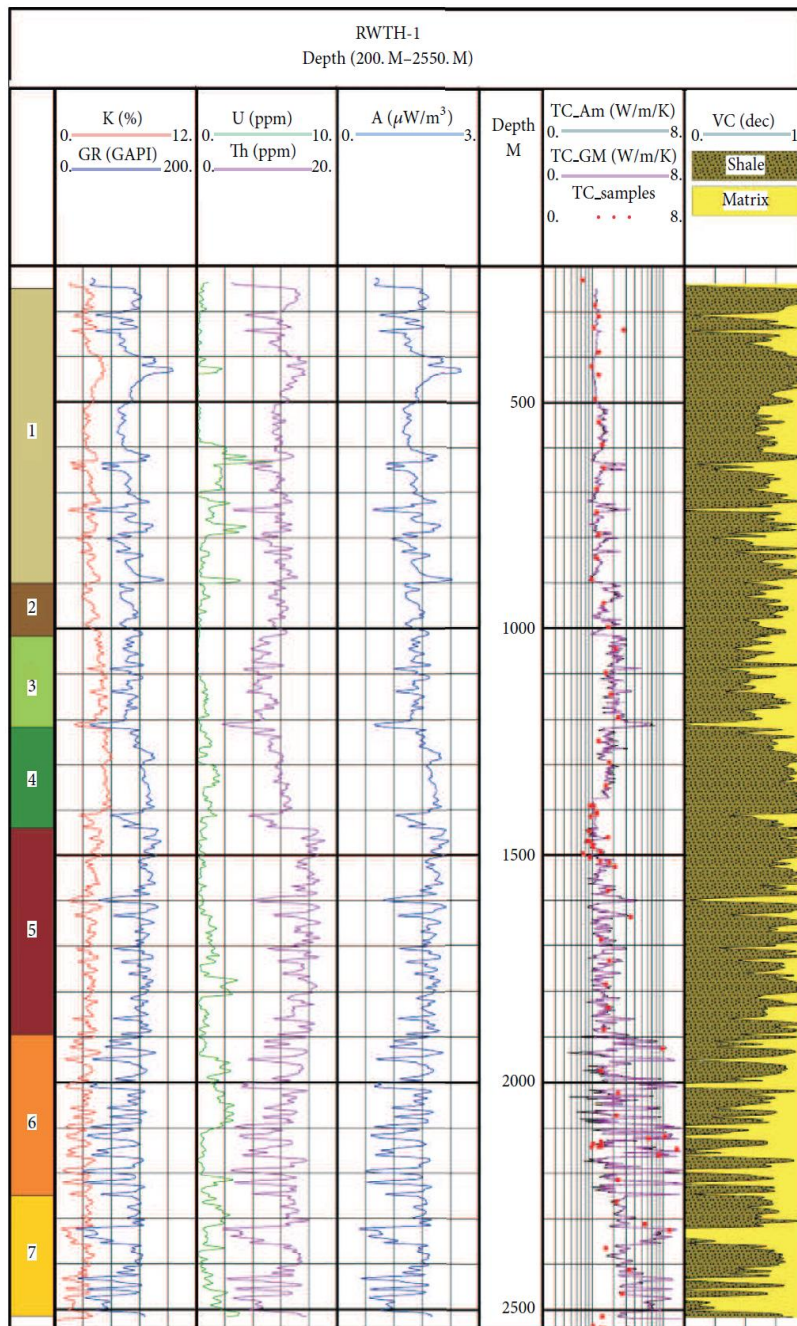


Figure 7. Thermo conductivity TC AM (arithmetic mean) and TC GM (geometric mean) and heat generation A are derived from the volume of fractions based on total (GR) and spectrum (K, U, Th); Colors indicate different borehole zones

3. Numerical cylindrical model

For the simulation of the influence of different parameters on the output heat exchanger from the heat exchanger and consequently on its thermal power, a finite difference method (FD) was used called SHEMAT (Simulator for HEat and MAss Transport) [10]. Due to the fact that the permeability of the layers is very low and the natural flows of groundwater are not detected, a cylindrical symmetrical model can be used. Due to symmetry, only 2D networks are sufficient (Figure 8). Constant properties of zone materials are specified for each network block. The properties of different geological zones are marked on the right [2]. The different properties of the heat exchanger zone are based on the geometry of the heat exchanger, as shown on the left side of Figure 8. The heat exchanger has four enclosures of different lengths. The total 2D network model includes a cylindrical body with a radius of 99.5m and a depth of 2973.5m. It is assumed that the geological zones are almost horizontal due to the low inclination of the layers in relation to the well of about 100. Fluid and heat flows are calculated via the interface by dividing the blocks (access to the hidden network).

It turned out that the heat exchanger affects the soil cooling in a radius of about 10m around the borehole [3]; therefore the radial environment is more than sufficient. The minimum size of a measuring cell of 5mm in each zone of special interest (input, output, housing) was used because of the required high accuracy at these locations.

The size of the network of the conveyor zone from the well to the surrounding walls increased with a factor of 1.5 which resulted in a maximum cell size of 25m. The number of cells is $91 \times 201 = 18291$ cells. For each budget step, it takes about 1 second. The image shows the model in comparison with the geological profile. The lithology column is simplified on units of 25m (maximum cell size). The radius and depth of the casing, as well as changes in lithology, are well represented.

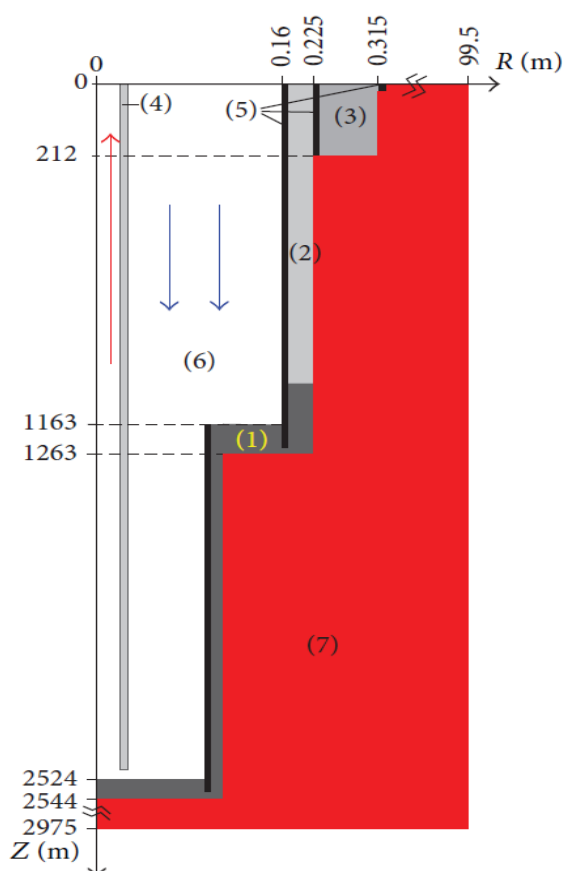


Figure 8. Used 2D cylindrical grid (radius 99.5m and depth 2973.5m) of the heat exchanger in different wall zones of the well. Thermal conductive cement (1), insulation cement (2), normal cement (3), inner tube (4), steel pipe (5), water (6) and surrounding borehole (7)

3.1. Model parameters

The wall permeability in the model was set to zero because of the extremely low porosity and the absence of water inflow during drilling and sampling. The flow of water in the inner tube, as well as between the inner and outer pipes is completely defined by constant volume flow. Since there are no layers with high specific heat capacity, the average value of specific heat capacity; $2.2\text{MJ}/(\text{m}^3\text{K}) \pm 20\%$ was used for surrounding walls (Figure 8) in simulations [11], [12]. Three outer pipes of steel tubes (Figure 8: (5)) have a specific heat capacity of $3.51\text{MJ}/(\text{m}^3\text{K})$. The specific values of the thermal capacity of the cement are $1.4\text{MJ}/(\text{m}^3\text{K})$ for insulation cement up to the depth of 1025m, $1.58\text{MJ}/(\text{m}^3\text{K})$ for thermal conductive cement from a depth of 1025m to the final depth of the well, and $1.65\text{MJ}/(\text{m}^3\text{K})$ for normal cement. The thermal conductivity of the cell's cells varies with the depth, according to the average thermal conductivity of the determined log (Figure 7). The inner tube, separating the cold water flowing from the hot water flowing upwards, needs to be insulated and have a realistic thermal conductivity of $0.1\text{W}/(\text{mK})$ unless otherwise stated. The inlet pipe has a thermal conductivity of $50\text{W}/(\text{mK})$ steel (Figure 8). The values for cement were given by Karat: $0.52\text{W}/(\text{mK})$ for insulation cement, $2.02\text{W}/(\text{mK})$ for thermal conductive cement and $1.21\text{W}/(\text{mK})$ for normal cement, under assuming that the shutdown is error-free [6].

As shown in Figure 7, heat generation A is less than $3\mu\text{W}/\text{m}^3$, on average only about $0.5\mu\text{W}/\text{m}^3$, and is therefore neglected in the model.

Based on measurements [13], a constant surface temperature from 100°C to 35°C is used in the model as the upper boundary condition of the surface of the surface. Constant specific heat flow is set as the lower limit state. He's welded. The German average of $69\text{mW}/\text{m}^2$ [14], $72\text{mW}/\text{m}^2$ is near the nearby Konzen bore [15]. The values specific heat flow of $110\text{mW}/\text{m}^2$ at a depth of 1312m and $90\text{mW}/\text{m}^2$ between 1791m-2291m are values for Peer and Soumagne wells [16].

3.2. Simulations and results

Here, the simulations and the resulting obtained temperature T_{out} from the heat exchanger placed in the well and the time interval for which a temperature greater than 55°C is reached which is necessary for the operation of the absorption air conditioner are described and analyzed. The size of the time step has a great effect on the duration of the simulation and the accuracy of the rapid temperature change; therefore, the simulation of the operation of the operation requires short-term steps for sufficient accuracy. This results in an extremely large countdown time (weeks).

3.2.1. The effects of heat conductivity of the inner tube. The thermal conductivity of the inner tube λ_{pipe} has a significant effect on the achieved output temperature and the corresponding thermal power P_T . In principle, the importance of isolation increases with decreasing the volume flow. This effect is important because of the longer time required to transfer heat from the water in the outer tube to the water in the inner tube. As shown in Figure 9, at a flow rate of $4\text{m}^3/\text{h}$, a reduction in thermal conductivity from $0.005\text{W}/(\text{mK})$ to $0.0001\text{W}/(\text{mK})$ insulation results in an increase in the maximum temperature T_{max} of less than 20K ; i.e. $0.005\text{W}/(\text{mK})$ is the optimum value. On the other hand, an increase of $0.05\text{W}/(\text{mK})$ reduces the time t ($T > 55^\circ\text{C}$) to achieve the required temperature greater than 55°C . According to [17], GRP pipes usually have a conductivity of $0.36\text{W}/(\text{mK})$. In Weggis (Switzerland), a steel pipe with double walls is in use, between which there is a vacuum of 0.02MPa . Its minimum thermal conductivity λ_{pipe} is $0.09\text{W}/(\text{mK})$, [18]. The latest GRP pipes have a thermal conductivity of $0.36\text{W}/(\text{mK})$. On the other hand, even with the best available insulation with a thermal conductivity of λ_{pipe} of about $0.1\text{W}/(\text{mK})$, the temperature losses are 19% to 31%. Therefore, as shown in Figure 9, only insulation with less than $0.1\text{W}/(\text{mK})$ is sufficient to maintain the required temperature for operation of the air conditioner. As shown in Figure 10, in the case of realistic insulation of $0.1\text{W}/(\text{mK})$, the temperature falls below the required minimum of 55°C , but after an uninterrupted operating time of $\frac{1}{2}$ days.

3.2.2. Effects of flow velocity. The water in the heat exchanger in the well may circulate with different flows $F(\text{m}^3/\text{h})$. The water retention time inside the pipe and the corresponding total circulation time are 1,0h and 11,7h for a flow of $10\text{m}^3/\text{h}$ and 1,9h and 23,4h for a flow of $5\text{m}^3/\text{h}$. Flow values F are directly related to the thermal power P_T of the heat exchanger of the well and are calculated as:

$$P_T = c_{pw} \rho_w F_w (T_{out} - T_{in}) \quad (3)$$

where c_{pw} is indicated with the thermal capacity of water, with ρ_w water density and with the T output and the input temperature of the heat exchanger, respectively. In order to see the effect on the output temperature, a volume flow change is simulated: $1\text{m}^3/\text{h}$, $4\text{m}^3/\text{h}$, $6\text{m}^3/\text{h}$, and $10\text{m}^3/\text{h}$. Isolation of $0,01\text{W}/(\text{mK})$ provides even 1/10 better thermal conductivity than the real heat conductivity of the inner tube.

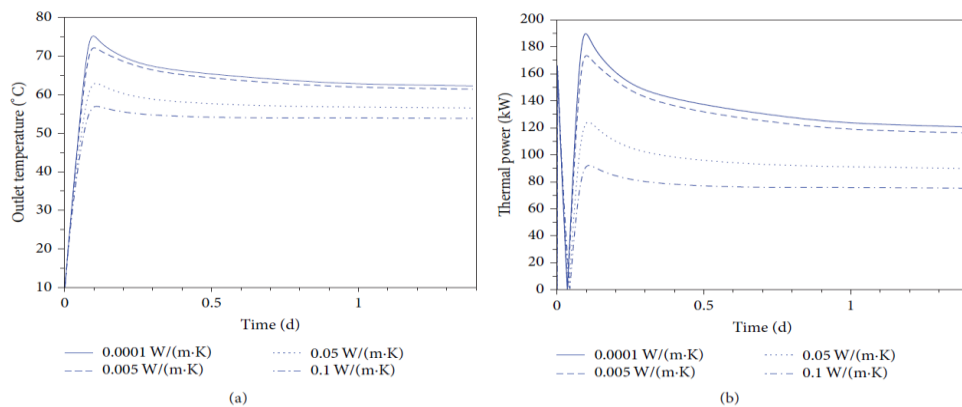


Figure 9. Variation of the temperature of the outgoing water and the heat energy of the heat exchanger in the well with time, for the different heat conductivity of the inner tube and for the continuous operation of the heat exchanger

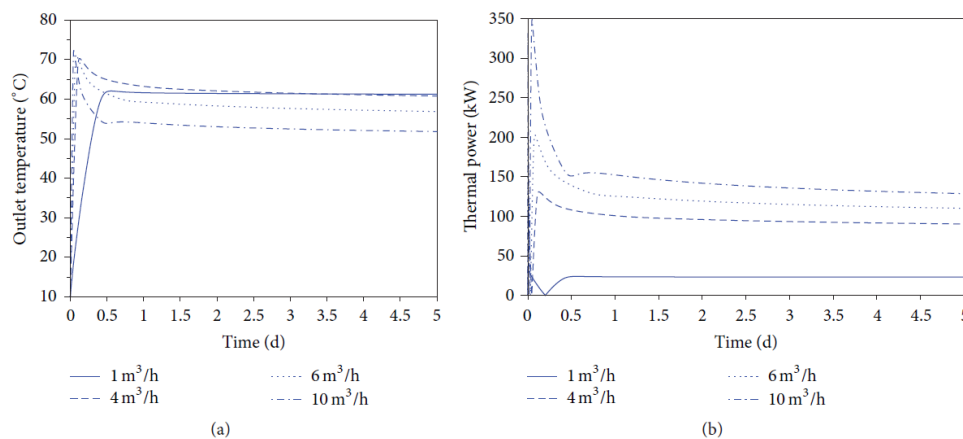


Figure 10. Behavior of the temperature of the outgoing water and heat energy of the heat exchanger with time, for different flows of water and for continuous operation

As shown in Figure 10, with a drop in insulation of 1/10, the temperature drop below is minimum required from 55°C and if the flow increases. After 5 days of continuous operation, the temperature and heat output are 52°C , 57°C , 60.5°C , and 61°C and 120kW , 110kW , 90kW and 20kW , respectively.

3.2.3. Thermal capacity effect tubing. The effect of the specific heat capacity of the inner tube, the specific heat capacity of c_p "windows", "district heating networks", "glass fiber reinforced plastics" and other materials were used in the simulation. These variations had no effect on T_{\max} and t ($T > 55^\circ\text{C}$).

3.2.4. Operational Cycle Effects. The previously described simulations have shown that the continuous operation of the heat exchanger will not bring the temperature needed for the operation of the absorption heat sink. Cyclical operations with heat extraction in the daytime and heat recovery were simulated to maximize the output temperature (Figures 11 and 12). The water flow is $3\text{m}^3/\text{h}$; a period of 6 hours of heat extraction is shifted with a period of 18 hours of heat recovery. Shorter extraction periods were ineffective, as it took 1h to remove cooled water from the inner tube. A low flow value has been selected to maintain a high temperature over a longer period of time. Large flow would have the opposite to cause too much cooling of the wall. Moreover, it turned out that even with the best insulated tubes, the temperature drop would occur during stopping. In continuous or cyclical operation, the temperature and heat output are about 49°C and 34°C to 51°C and 29kW and 20kW to 35kW , respectively (negative values are due to the start of cold water after restarting the system).

Figure 11 shows the output temperature and the corresponding thermal power after 20 years of operation for cyclic and continuous flow of $3\text{m}^3/\text{h}$ and for a four-day interval of operation. Figure 12 shows a long-term simulation over a period of 10 to 20 years with a flow of $3\text{m}^3/\text{h}$ for continuation of operation as well as for a daily working cycle consisting of 6h pump operation and 18h recuperation.

The maximum and minimum temperatures in cyclic operation are displayed. It is shown that even after 20 years of operation, the heat exchanger in the well did not stop the loss of efficiency. In the first years, the reduction in thermal power and temperature is the highest, and then remains stable after 20 years of operation. The water temperature is sufficient for direct heating in the winter. It is important to consider that the constant input temperature is 40°C . The temperature difference between the maximum cyclic and non-cyclic temperature is 20°C . The time required is increased until hot water flows from the inner tube. Different flows are simulated for cyclical operations consisting of 6h pumping, followed by 18h - recovery with real thermal conductivity of inner tube $\lambda_{\text{pipe}} = 0.1\text{W}/(\text{mK})$.

The cycle curves in Figures 11 and 12 show that the required minimum temperature of 55°C has never been achieved.

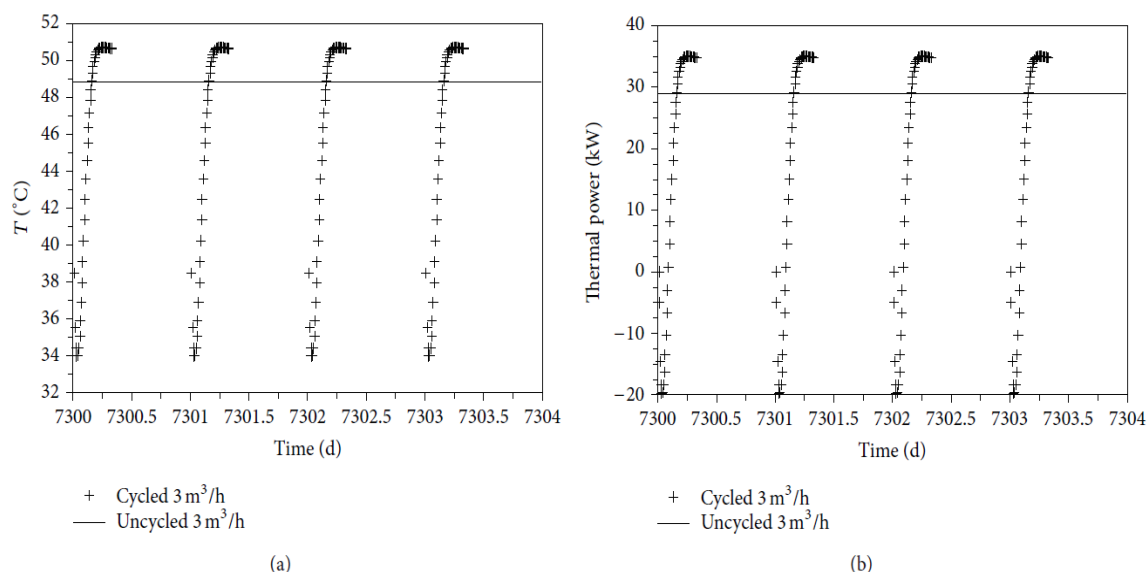


Figure 11. Output water temperature and associated heat output relative to the time after 20 years of operation for cyclic and continuous flow of $3\text{m}^3/\text{h}$

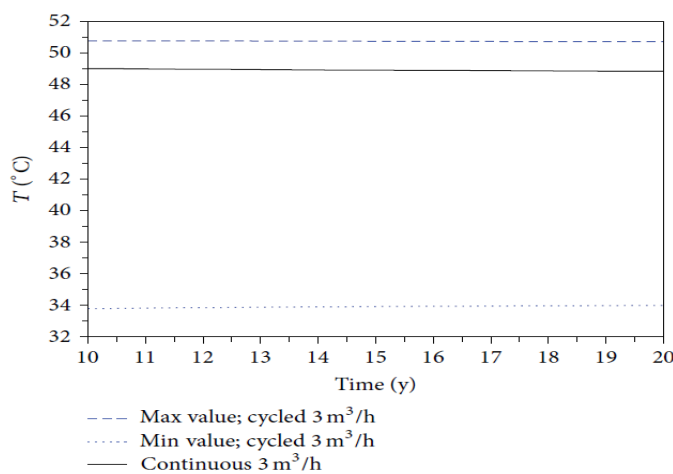


Figure 12. Maximum and minimum temperatures for cyclic and continuous work, with a constant flow of $3\text{ m}^3/\text{h}$ and a time interval between 10 and 20 years of operation

3.2.5. Simulation of the Crypto Control Unit for the Super C category building. It is clear from the above figures that it is impossible to achieve, given the currently available insulation for the inner tube, the temperature of 55°C required for the operation of the adsorption chiller. Even in the case of better insulation in the future, flow rates are limited to reach the required temperature.

In addition to the adsorption refrigerant, two compressor cooling units are planned with a capacity of 130 kW . The adsorption chiller works with a coefficient of effect (COP) of $0.38\text{--}0.63$ for lower temperatures, $55^\circ\text{C}\text{--}85^\circ\text{C}$ followed [19]. Therefore, in order to cool the building with 1 kW , the adsorption chiller should use a more/less $1/0.38=3\text{ kW}$ geothermal *energy* resulting in 4 kW of additional heat, which contributes to global warming of the environment. Therefore, even with the future improvement of the isolation material, we can wonder if this is a sustainable way of cooling, it is probably not. In any case, according to German regulations, the maximum cooling power required is limited to the ambient temperature of 28°C . In Aachen, this temperature will be 37 hours a year. Also, the need for cooling above 20°C is 580 hours a year in Aachen [19]. In case the adsorption refrigeration unit can not meet, it can only operate 50% of the total cooling power, which corresponds to a cooling period of 190 hours per year.

As for the heating of the building, the total heat transfer coefficient (U -value) in the building is 7.9285 kW/K [19]. With this value, it is possible to calculate the maximum required heating power to maintain the room temperature of 18.3°C , at an outside temperature of 12°C . Installed heating bodies are: standard radiators ($70^\circ\text{C}\text{--}35^\circ\text{C}$), floor heating ($32^\circ\text{C}\text{--}30^\circ\text{C}$) and concrete core ($28^\circ\text{C}\text{--}25^\circ\text{C}$). This high-temperature acceptance of the temperature allows the storage of large amounts of heat in the building and the reduction of the return temperature of the return water from the building to 25°C .

Air temperatures recorded at Euro planetarium Genk (60km from Aachen) in 2005, every 30 minutes, were taken to simulate the required thermal power over time for the Super C building (Figure 13 (1)). The required power (Figure 13 (4)) and the temperature of the outgoing water from the building (25°C) are used as input parameters for the simulation of the heat exchanger in a deep well. Figure 13 (2) shows the required flow value for a semi-annual simulation. The flow through the heat exchanger is changed every 30 minutes until the required power is reached. It is clear that the output temperature (Figure 13 (3)) slowly decreases over time, but the heat output is satisfactory (Figure 13 (4)).

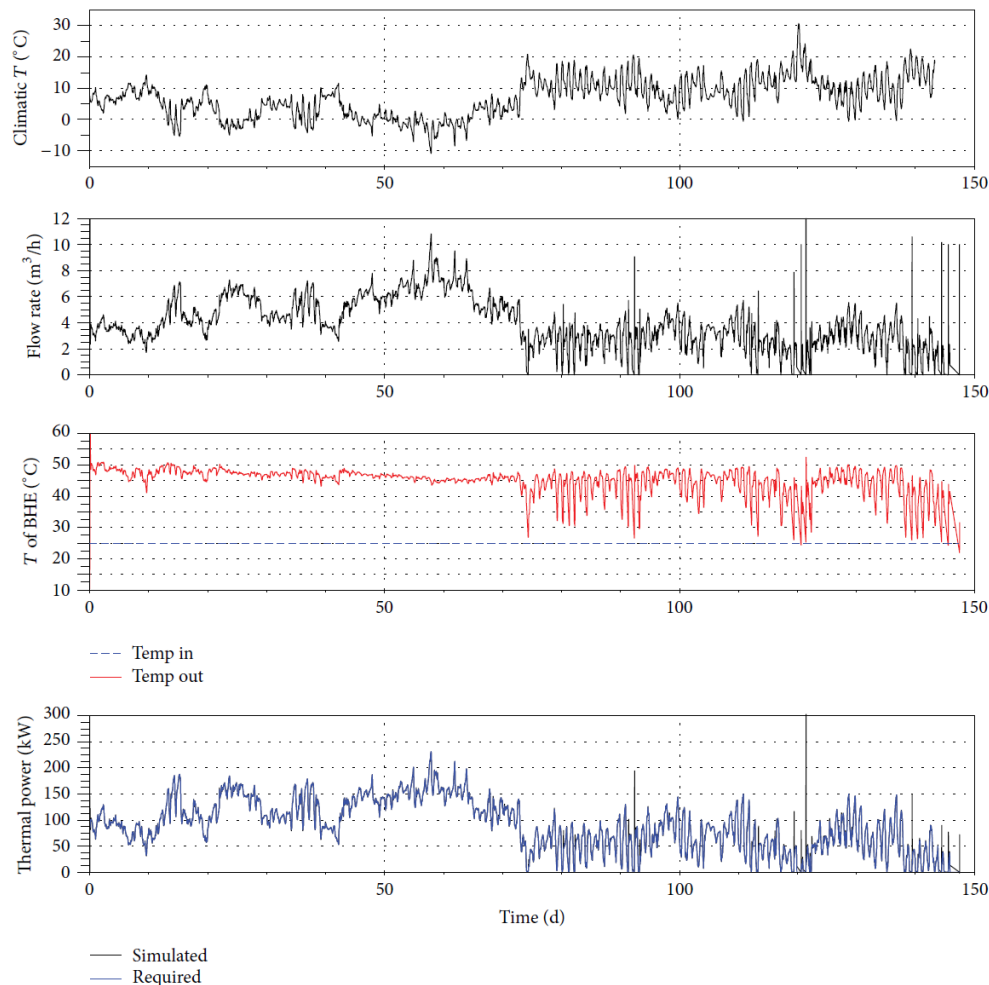


Figure 13.

With actual temperature data in the first half of 2005, the need for heating and cooling for the Super C building was calculated, using a mean value of U 7.9285kW/K [19]. The assumption is that the heating bodies in the building return water with a constant temperature of 25°C which will be the input water temperature in the BHE. Output temperature and water flow are simulated in BHE. The required heat power in the first half of the year is compared with the calculated thermal energy required by the building.

4. Final result

In 2008, the building of the Super C class (Figure 1) was officially connected to the city heating, but with the intention of using the borehole for geothermal heating in the future. At the time, there were still problems in finding suitable insulation material for the inner tube. Finally, in 2011, RWTH Aachen decides that the operation of a deep-water drill shaft will not be economical due to the high additional costs of the thermal insulation of the inner tube.

5. Conclusion

In order to heat or cool the A-Class building in the energy class "Super C", in the city center of Aachen, Germany, it is necessary to have 40°C for direct heating of the building in winter, while

cooling air for the building with adsorption cooling unit requires a temperature of minimum 55°C. Measurements and calculations for deep-coaxial heat exchanger (CBHE) depth of 2500m, with a maximum temperature in a well at 85°C at that depth of 2500m, reveals the contradiction between the maximum required temperature for the adsorption air conditioning unit and the maximum thermal power. Numerical calculations indicate that only in a short period of time in a cyclical operating mode, the borehole can supply at the same time the required temperature of 55°C and a heat output of 120kW, with an input temperature of 40°C and a flow of 3m³/h. However, after 20 years of operation, it has been shown that the temperatures are too low for the correct operation of the adsorption cooling unit. During the winter, the heat exchanger can supply the building with sufficient amount of heat, with temperatures from 25°C to 55°C and throughput to a maximum of 10m³/h. Also, numerical calculations indicate the great importance of isolating the inner tube. This requires a very expensive inner tube, which in turn results in the fact that the total heat exchanger for this well in Aachen is economically unsustainable.

References

- [1] Dijkshoorn L, Speer S and Pechinig R 2013 Measurements and Design Calculations for a Deep Coaxial Borehole Heat Exchanger in Aachen, *International Journal of Geophysics* 916541
- [2] Oesterreich B, Trautwein U and Lundershausen S 2005 Die geothermiebohrung RWTH-1, VAG—Vereinigung Aachener Geowissenschaftler e.V. Infoblatt
- [3] Signorelli S 2004 *Geoscientific investigations for the use of shallow low-enthalpy systems*, ETH Zürich University, Zürich, Switzerland, Doctoral Thesis
- [4] ***1997 *Akkupyc Manual*, Micromeritics Instrument Corporation, Norcross, Ga, USA
- [5] ***2005 *Instrument Manual TCS—High Precision Thermal Conductivity Measurement*, Lippmann and Rauen GbR, Schaufling, Germany
- [6] Speer S 2005 *Design calculations for optimising of a deep borehole heat-exchanger*, Institute of Applied Geophysics, RWTH Aachen University, Aachen, Germany, M.S. Thesis
- [7] Çermak V, Bodri L, Rybach L and Buntebarth B 1990 Relationship between seismic velocity and heat production: comparison of two sets of data and test of validity, *Earth and Planetary Science Letters* **99**(1-2) 48-57
- [8] Rybach L 1978 The relationship between seismic velocity and radioactive heat production in crustal rocks: an exponential law, *Pure and Applied Geophysics* **117** (1-2) 75-82
- [9] Bücker C and Rybach L 1996, A simple method to determine heat production from gamma-ray logs, *Marine and Petroleum Geology* **13**(4) 373-375
- [10] Clauser C 2003 *Numerical Simulation of Reactive Flow in Hot Aquifers*, Springer, Berlin, Germany
- [11] Beck A 1998 *Methods for determining thermal conductivity and thermal diffusivity, in Handbook of Terrestrial Heat Flow Density Determination*, (R Haenel, L Rybach and L Stegena, Eds.) Kluwer Academic Publishers, Norwell, Mass, USA
- [12] Vosteen H D and Schellschmidt R 2003 Influence of temperature on thermal conductivity, thermal capacity and thermal diffusivity for different types of rock, *Physics and Chemistry of the Earth* **28**(9-11) 499-509
- [13] Clauser C 1984 A climatic correction on temperature gradients using surface-temperature series of various periods, *Tectonophysics* **103**(1-4) 33-46
- [14] Schellschmidt R, Hurter S, Forster A and Huenges E 2002 *Atlas of Geothermal Resources in Europe*, Office for Official Publications of the European Communities, Brussels, Belgium
- [15] Karg H 1995 *Untersuchung des Temperatursfeldes im Untergrund der Region Aachen-Maastricht-Lüttich*, Applied Geophysics and Geothermal, Aachen University, Aachen, Germany, Master Thesis
- [16] Verkeyn M 1995 *Bepaling van de Warmestroomdichtheid in België en de verkenning naar de mogelijkheden en de beperkingen* (Determination of the Specific Heat Flow in Belgium with possibilities and limitations), University Leuven Belgium, Master Thesis

- [17] Summa F, Benner L and Otto F 2005 *Tagung für Ingenieurgeologie Erlangen, Geothermie unter geotechnischen und wirtschaftlichen aspekten*
- [18] Kohl T, Brenni R and Eugster W 2002 System performance of a deep borehole heat exchanger, *Geothermics* **31**(6) 687-708
- [19] ***2004 *Superc entwurfplanung, unterlagen zur hubau*, Tech. Rep. 33239, Arup GmbH, New York, NY USA